

This is the **accepted version** of the journal article:

Francàs, Laia; Burns, Eric; Steier, Ludmilla; [et al.]. «Rational design of a neutral pH functional and stable organic photocathode». *Chemical Communications*, Vol. 54, Issue 45 (June 2018), p. 5732-5735. DOI 10.1039/c8cc01736k

This version is available at <https://ddd.uab.cat/record/290958>

under the terms of the  **CC BY-NC-ND** license

Rational design of a neutral pH functional and stable organic photocathode

Received 00th January 20xx,
Accepted 00th January 20xx

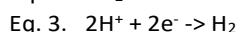
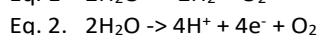
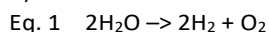
Laia Francàs,^{‡a*} Eric Burns,^{‡a} Ludmilla Steier,^a Hyojung Cha,^a Lluís Solà-Hernández,^b Xiaoe Li,^a Pabitra Shakya Tuladhar,^a Roger Bofill,^b Jordi García-Antón,^b Xavier Sala,^b James R. Durrant^{a*}

DOI: 10.1039/x0xx00000x

www.rsc.org/

In this work we lay out design guidelines for catalytically more efficient organic photocathodes achieving stable hydrogen production in neutral pH. We propose an organic photocathode architecture employing a NiO hole selective layer, a PCDTBT:PCBM bulk heterojunction, a compact TiO₂ electron selective contact and a RuO₂ nanoparticle catalyst. The role of each layer is discussed in terms of durability and function. With this strategically designed organic photocathode we obtain stable photocurrent densities for over 5 h and discuss routes for further performance improvement.

Solar energy could provide a clean and renewable source of energy.¹ However, harvesting solar energy in a useable form remains one of the major challenges that humanity is now facing. One strategy is the storage of this solar energy in the form of chemical bonds through the production of hydrogen, the energy carrier, and oxygen from water (eq 1), using a tandem photoelectrochemical device. Such devices consist of a photoanode (oxidation, eq. 2) and photocathode (reduction, eq. 3).²



One of the major challenges when designing such tandem cells is the matching of both photoelectrodes in terms of pH stability, complementary absorbance and energetics.³ Traditionally inorganic semiconductors have been used for such electrodes, however the fine tuning of their properties is often synthetically challenging.⁴ To overcome this limitation, organic semiconductors have started to attract significant interest in recent years, due to their readily tuneable energetics and optical properties.⁵⁻⁷ Making use of these

properties, together with suitable functional layers (such as selective hole/electron transport layers and catalysts), efficient organic photocathodes have been demonstrated.⁸⁻¹² The rational design of the different functional layers of such organic photocathodes is essential for the optimisation of device performance (higher photocurrent at lower applied potential and improved stability). With the aim of analysing recent progress in this regard, we structured and summarised relevant literature on organic photocathodes in Table S1. From this table we made two major observations: most of the organic photocathodes are (i) based on P3HT:PCBM blends and (ii) greatly suffer from degradation under operational conditions. In the photovoltaic field it is well known that P3HT based blend shows limited voltage output, limiting its final efficiency to 3-4%.¹³ Hence, photocathodes using this blend are also limited in their output. So we need to find other materials to replace P3HT. In addition of the very few examples that demonstrate reasonable operational stabilities, photocathodes protected by TiO₂ grown by atomic layer deposition (ALD) stand out as showing operational stability for more than 3.5 hours.¹⁴ This work is focused on the development of new organic photocathode designs yielding higher photovoltages and significantly improved operational stabilities, achieved by combining the ALD TiO₂ protection layer approach with the rational design of suitable organic photoactive layer and hole transport layer.

Herein, we report organic photocathodes yielding high photovoltages and photocurrent densities for hydrogen evolution with stabilities exceeding 5 hours under 1 sun (AM 1.5G) operation in pH 7 phosphate buffer. In addition, the excellent performance of this photocathode meets the required conditions such as stability under the same pH or energy alignment for coupling to state-of-the-art BiVO₄ photoanodes as needed for tandem photoelectrochemical cells.¹⁵

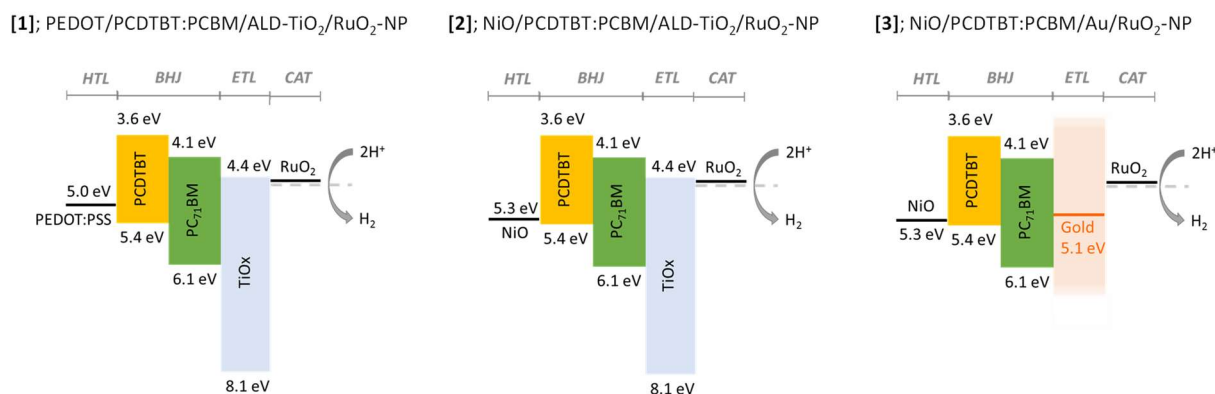
Scheme 1 depicts the three different configurations of organic photocathodes studied in this work based on PCDTBT:PCBM blends and RuO₂ catalysts.

^a Department of Chemistry, Imperial College London, South Kensington Campus, London, SW7 2AZ, United Kingdom.

^b Departament de Química, Universitat Autònoma de Barcelona, Cerdanyola del Vallès, 08193 Barcelona, Spain.

[‡] The two authors contributed equally to this research work

Electronic Supplementary Information (ESI) available: [details of any supplementary information available should be included here]. See DOI: 10.1039/x0xx00000x



Scheme 1. Schematic representation of the organic photocathodes layers and the energetic levels of the photocathodes used herein and their correspondent labelling. ETL= electron transport layer, BHJ = organic bulk heterojunction, HTL= hole transport layer, CAT= Catalyst.

Each photocathode comprises: (1) an organic bulk heterojunction (BHJ) layer to absorb light and drive photoinduced exciton separation between an electron donor polymer and an electron acceptor small molecule; (2) a hole transport layer to help hole transfer selectively from the BHJ layer to an ITO anode; (3) an electron transport layer to selectively transfer electrons from the BHJ layer to (4) a catalyst layer which performs the catalytic reduction of protons at the liquid interface to generate hydrogen (eq 3). The Layers (1)-(3) can be found in conventional photovoltaic device configuration and are responsible for the photoinduced charge carrier generation and separation. The presence of the catalytic layer (4) is one of the main differences between the photocathode and the organic photovoltaics (OPVs) configuration.

As discussed above, most organic photocathodes reported in the literature (Table S1) use P3HT:PCBM bulk heterojunctions, which limits its final onset voltage for photocatalysis. For this reason we chose for the first time PCDTBT:PCBM (Chart 1) as a suitable absorber blend. OPV devices based on PCDTBT:PCBM yield efficiencies of 6-7%, in contrast to the 3-4% efficiencies¹³ for OPVs based on P3HT. This improvement is primarily due to its open circuit voltage of 0.8 eV, resulting from PCDTBT's deeper HOMO level (Supporting information Figure S4). In addition, PCDTBT:PCBM solar cells have been reported to display longer *in operando* lifetimes.¹⁶

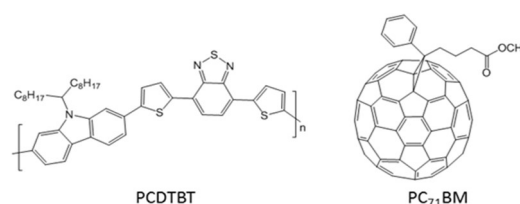
Current density - potential (J-V) curves of our organic photocathodes in pH 7 phosphate buffer are presented in Figure 1. Firstly, we focus on photocathode **[1]** (PEDOT:PSS/PCDTBT:PCBM/ALD-TiO₂/RuO₂-NP), green trace in Figure 1. As can be observed, this is the best performing configuration in terms of photocurrent onset and amount of photocurrent when compared to photocathode designs **[2]** (NiO/PCDTBT:PCBM/ALD-TiO₂/RuO₂-NP) and **[3]** (NiO/PCDTBT:PCBM/Au/RuO₂-NP) (Scheme 1). Remarkably, this photocathode configuration provides a photovoltage of 0.7 V that is very close to the obtained open circuit voltage (V_{oc}) of the OPV counterpart. When comparing these

performance data (Table S1, entry 2) against previous literature [Table S1, entries 26 and 34, which use PEDOT as hole transport layer (HTL) and TiO₂ as an electron transport layer (ETL)], we can observe that the onset of the photocurrent is shifted 0.2-0.5 V towards more positive potentials when P3HT is substituted by PCDTBT **[1]**. This difference is of similar magnitude to the shift in V_{oc} of their OPV device counterparts (Figure S4). In addition, higher photocurrent is measured when PCDTBT is used, also in accordance with the higher short circuit current measured in its photovoltaic device. Hence the enhanced photocathode **[1]** behaviour reflects the improved fundamental bulk heterojunction properties also observed in OPV devices.

As can be observed in Figure 2a, green trace, despite this improved efficiency, the stability of photocathode **[1]** is relatively poor; the activity decreased by 95% after 90 min of photoelectrolysis under 1 sun illumination at 0 V vs RHE, similar to analogous systems in the literature (Entry 34, Table S1). PEDOT:PSS (henceforth referred to as PEDOT), used as the HTL in this photocathode, is known to be hygroscopic and structurally unstable in aqueous conditions.

To achieve better operational stabilities, previous work by Haro *et al.* used a cross-linked PEDOT layer (Entry 26, Table S1). However, their devices suffered from significantly lower photocurrent densities. Other works have employed more stable inorganic HTLs in organic photocathodes but long-term stabilities could not be achieved with this strategy alone (entries 4, 5, 6 and 11, Table S1). From Table S1 in supplementary information we identified TiO₂ and especially the ALD-TiO₂ as a suitable ETL.^{8, 10} Hence, our strategy towards a stable organic photocathode lies in the combination of stable HTLs with efficient and stabilising ETLs. In the paper of Steier *et al.* ALD-TiO₂ was deposited on P3HT:PCBM which is one of the few BHJs not degrading under thermal annealing.

Chart 1. Structures of the molecules used in this work.



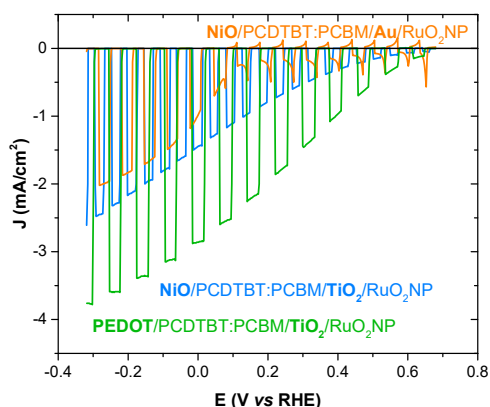
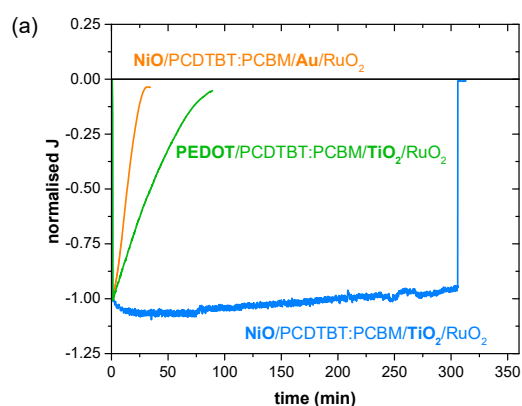


Figure 1. Chopped J-V curves under 1 sun illumination (Xe-lamp) in a three electrode cell pH 7 (0.1 M phosphate buffer) of different photocathodes configuration, changing electron and hole transfer layers: PEDOT/PCDTBT:PCBM/TiO₂-ALD/RuO₂-NP; **[1]** (green); NiO/PCDTBT:PCBM/TiO₂-ALD/RuO₂-



NP; **[2]** (blue); NiO/PCDTBT:PCBM/Au/RuO₂-NP; **[3]** (Orange).

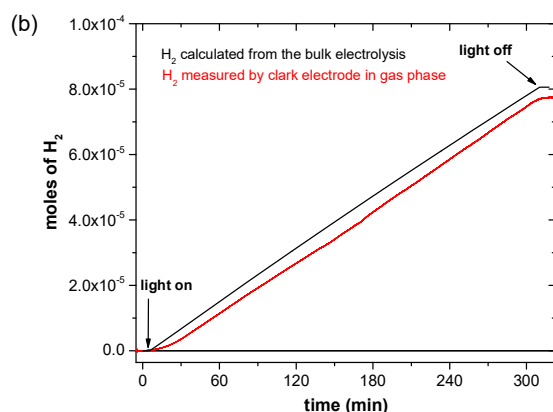


Figure 2. (a) Bulk electrolysis under 1 sun illumination (Xe-lamp) at 0 V vs RHE of applied potential in a three electrode cell at pH 7 (0.1 M phosphate buffer) of different photocathodes configuration: PEDOT/PCDTBT:PCBM/TiO₂-ALD/RuO₂-NP; **[1]** (green); NiO/PCDTBT:PCBM/TiO₂-ALD/RuO₂-NP; **[2]** (blue); NiO/PCDTBT:PCBM/Au/RuO₂-NP; **[3]** (Orange). (b) Moles of produced hydrogen measured by Clark electrode in the gas phase (red) and the amount of hydrogen calculated

from the bulk electrolysis current (black) for the photocathode **[2]** (0.6 cm²).

Here, we achieved deposition of ALD-TiO₂ on the thermally sensitive PCDTBT:PCBM photoactive blend demonstrating that low-temperature ALD-TiO₂ is generally a suitable ETL in organic photocathodes, even in those employing thermally sensitive BHJs.²² However, it is apparent from Figure 2a that photocathode **[1]**, with PEDOT as HTL, shows a dramatic drop in photocurrent in less than an hour. This indicates that even ALD-TiO₂ does not form a sufficiently good water barrier for strongly hygroscopic HTL materials.

Hence, we sought a more stable HTL material. In OPV devices, replacement of PEDOT with NiO as an alternative HTL has been shown to improve device stability under humidity exposure. With this in mind, the PEDOT layer was replaced in our photocathode by a layer of NiO to generate the photocathode NiO/PCDTBT:PCBM/ALD-TiO₂/RuO₂-NP, **[2]** (Scheme 1). As can be observed in comparing the green **[1]** and blue **[2]** traces within Figure 1, the photocurrent onset potential is not altered by the change in HTL, however the overall performance was reduced in terms of photocurrent maximum and shape of the J-V curve. This reduction can be associated with the higher resistivity of our NiO layer in comparison to our PEDOT and is in agreement with the increased series resistance visible in the J-V curves of the OPV counterparts (Figure S5).¹⁷⁻¹⁹

Although we suffer from a decrease in maximum photocurrent with our NiO-based organic photocathodes (≤ 2 mA cm⁻² at 0 V_{RHE} for **[2]** and **[3]**), we could achieve a dramatic improvement in operational stability with photocathode **[2]**, showing less than 10% photocurrent loss over 5 h under 1 sun illumination at 0 V vs RHE (Figure 2a). This corresponds to being one of the most stable high-performance organic photocathodes for H₂ production in neutral pH reported to date (Table S1).

We note that this remarkable result could only be achieved through a combination of NiO as a chemically more stable HTL in water and an ALD-TiO₂ ETL for good charge extraction, electrode protection and catalyst support. For example, in a comparison with a Au contact replacing the ALD-TiO₂ ETL, Figure 1 shows the impact of a selective TiO₂ layer on the extracted photovoltage: it is apparent from the high spikes in the chopped J-V curve of the Au-based photocathode **[3]** that charges are lost due to recombination at the BHJ/Au/catalyst interfaces. In contrast, no spikes are observed with the TiO₂ electron selective layer, indicative of suppressed recombination losses. Moreover, the ALD-TiO₂ layer dramatically enhances the stability of the NiO based photocathode **[2]** (Figure 2a), which might be due to its function as protection layer and suitable catalyst support. Hence, a good ETL, in both energetics and stability terms, is necessary to obtain efficient photocathodes with high photovoltages.

Finally, we turn to discuss the role of the catalyst layer. In this work, we used small amounts of spin-coated RuO₂ nanoparticles, "RuO₂-NP" (See supporting information Figure S6). RuO₂ is black, so the use of low catalyst loadings is

advantageous in minimising absorption losses under front illumination conditions. As shown in Figure S7, we could achieve identical photocurrent densities with photocathode [2] for both illumination directions (illuminating from the ITO side or from the catalyst side). This is a result of low RuO₂ nanoparticle loadings required for our NiO/PCDTBT:PCBM/TiO₂ photocathodes to be efficient as well as the transparent HTL and ETL employed in our work. Illuminating the photocathode from the catalyst side (front side) is particularly useful as it allows for the reduction of ionic resistance losses in a tandem device. Contrary to most of the catalysts for H₂ production, RuO₂ also presents the same performance at pH 1 and at pH 7, which makes it an excellent candidate to work with state-of-the-art BiVO₄ based photoanodes (Figure S8). In addition, this electrolyte is posing less hazardous risks than working at strong alkaline or acidic pH, thus facilitating its practical implementation.

The optimised photocathode [2] employed in this study attains high activities (26 μmoles of H₂*h⁻¹*cm⁻²) over at least 5 hours of operation under 1 sun illumination (< 10% loss over 5 hours), with a constant Faradaic efficiency for hydrogen generation of 98% (see Figure 2b and supporting information for details). The stability of this photocathode was found to be further improved when working at lower light intensities (Figure S9), retaining 100% of initial performance over 5 hours operation under 0.1 sun irradiation. Longer term stability demonstrates up to 10 hours of activity with a 20% loss of activity during the second 5 hours of photoelectrolysis (Figure S10).

In conclusion, this outstanding operational stability and photocatalytic activity of our organic photocathodes was achieved through the rational design of blend, electron extracting, hole extracting and catalyst layers: (i) Through the choice of the PCDTBT:PCBM bulk heterojunction we were able to extract high photovoltages, leading to one of the best photocurrent onset potentials for hydrogen evolution with organic photocathodes reported to date. (ii) Furthermore, we succeeded in depositing TiO₂ by low-temperature ALD on the thermally sensitive PCDTBT:PCBM photoactive blend and showed its important role as a charge extraction layer in the organic photocathode. (iii) The substitution of PEDOT by NiO as HTL was essential to the stability of the photocathode in water. (iv) Finally, through the use of small RuO₂-NP loadings and transparent HTL as well as ETL, we bring forward an all-transparent organic photocathode with excellent operation under front and back side irradiation, making it highly suitable for tandem applications.

Following the key design guidelines presented in this work, further development of more efficient and stable organic photocathodes could be achieved through, for example, stable organic blends offering even higher photovoltages and stable but more conductive HTLs.

Conflicts of interest

There are no conflicts to declare.

Acknowledgements

We kindly thank the laboratory of photonics and interfaces (EPFL, Switzerland) for the permission to use their ALD setup. We acknowledge financial support from the European Research Council (project Intersolar 291482), K.A.U.S.T. (Project OSR-2015-CRG4-2572), and MINECO/FEDER (CTQ2015-64261-R). L.F. thanks the EU for a Marie Curie fellowship (658270). J. G.-A. acknowledges the Serra Hünter Program.

Notes and references

- N. S. Lewis, *Science*, 2016, **351**, 19201-19209.
- M. R. Shaner, H. A. Atwater, N. S. Lewis and E. W. McFarland, *Energy Environ. Sci.*, 2016, **9**, 2354-2371.
- K. Sivula and R. van de Krol, *Nat. Rev. Mater.*, 2016, **1**, 15010.
- P. V. Kamat and J. Bisquert, *J. Phys. Chem. C*, 2013, **117**, 14873-14875.
- R. Godin, Y. Wang, M. A. Zwiijnenburg, J. Tang and J. R. Durrant, *J. Am. Chem. Soc.*, 2017, **139**, 5216-5224.
- S. Holliday, R. S. Ashraf, A. Wadsworth, D. Baran, S. A. Yousaf, C. B. Nielsen, C.-H. Tan, S. D. Dimitrov, Z. Shang, N. Gasparini, M. Alamoudi, F. Laquai, C. J. Brabec, A. Salleo, J. R. Durrant and I. McCulloch, *Nat. Commun.*, 2016, **7**, 11585.
- R. S. Sprick, J.-X. Jiang, B. Bonillo, S. Ren, T. Ratvijitvech, P. Guiglian, M. A. Zwiijnenburg, D. J. Adams and A. I. Cooper, *J. Am. Chem. Soc.*, 2015, **137**, 3265-3270.
- A. Guerrero, M. Haro, S. Bellani, M. R. Antognazza, L. Meda, S. Gimenez and J. Bisquert, *Energy Environ. Sci.*, 2014, **7**, 3666-3673.
- T. Bourgeteau, D. Tondelier, B. Geffroy, R. Brisse, R. Cornut, V. Artero and B. Jusselme, *ACS Appl. Mater. Interfaces*, 2015, **7**, 16395-16403.
- T. Bourgeteau, D. Tondelier, B. Geffroy, R. Brisse, S. Campidelli, R. Cornut and B. Jusselme, *J. Mater. Chem. A*, 2016, **4**, 4831-4839.
- H. C. Rojas, S. Bellani, F. Fumagalli, G. Tullii, S. Leonardi, M. T. Mayer, M. Schreier, M. Gratzel, G. Lanzani, F. Di Fonzo and M. R. Antognazza, *Energy Environ. Sci.*, 2016, **9**, 3710-3723.
- S. Esiner, R. E. M. Willems, A. Furlan, W. Li, M. M. Wienk and R. A. J. Janssen, *J. Mater. Chem. A*, 2015, **3**, 23936-23945.
- M. T. Dang, L. Hirsch and G. Wantz, *Adv. Mater.*, 2011, **23**, 3597-3602.
- L. Steier, S. Bellani, H. C. Rojas, L. Pan, M. Laitinen, T. Sajavaara, F. Di Fonzo, M. Gratzel, M. R. Antognazza and M. T. Mayer, *Sustainable Energy Fuels*, 2017, **1**, 1915-1920.
- T. W. Kim and K.-S. Choi, *Science*, 2014, **343**, 990-994.
- C. H. Peters, I. T. Sachs-Quintana, J. P. Kastrop, S. Beaupré, M. Leclerc and M. D. McGehee, *Adv. Energy Mater.*, 2011, **1**, 491-494.
- M. D. Irwin, D. B. Buchholz, A. W. Hains, R. P. H. Chang and T. J. Marks, *Proc. Natl. Acad. Sci.*, 2008, **105**, 2783-2787.
- S. Wheeler, F. Deledalle, N. Tokmoldin, T. Kirchartz, J. Nelson and J. R. Durrant, *Phys. Rev. Applied*, 2015, **4**, 024020.
- Z. Yu, Y. Xia, D. Du and J. Ouyang, *ACS Appl. Mater. Interfaces*, 2016, **8**, 11629-11638.
- A. Paracchino, N. Mathews, T. Hisatomi, M. Stefiik, S. D. Tilley and M. Gratzel, *Energy Environ. Sci.*, 2012, **5**, 8673-8681.
- B. Seger, S. D. Tilley, T. Pedersen, P. C. K. Vesborg, O. Hansen, M. Gratzel and I. Chorkendorff, *J. Mater. Chem. A*, 2013, **1**, 15089-15094.

22. Z. Li, K. Ho Chiu, R. Shahid Ashraf, S. Fearn, R. Dattani, H. Cheng Wong, C.-H. Tan, J. Wu, J. T. Cabral and J. R. Durrant, *Scientific Reports*, 2015, **5**, 15149.